RESEARCH ARTICLE **Open Access**

A measurement system for the bicycle crank angle using a wireless motion sensor attached to the crank arm

Tomoki Kitawaki[1] ✉ **& Hisao Oka**[1]

Abstract

In this study, we propose a system for measuring the rotational angle of a bicycle crank arm. This system consists of a wireless motion sensor with bi-axial acceleration and angular velocity sensors attached to the crank arm. Rotational angles measured by the motion sensor were compared with data from a motion capture system. We found the RMS (root-mean-square) error for the bicycle crank angle was 0.339 ± 0.115 degrees (mean ± SD), and the angular velocity RMS error normalized by the average angular velocity was 0.655 ± 0.217 %. Using the proposed motion sensor system, we were able to measure the rotational angle and angular velocity of the bicycle crank to the same accuracy and high frequency as the motion capture system. Furthermore, we demonstrate it is possible to precisely obtain the rotational crank angle to evaluate fluctuations of crank angular velocity.

Keywords: motion sensor, wireless sensor, crank arm angle, angular velocity, bicycle pedaling.

✉ **Contact:** kitawaki@md.okayama-u.ac.jp (T. Kitawaki)

[1] Okayama University, Graduate School of Health Sciences, Okayama, Okayama, Japan

Received: 06 June 2013. Accepted: 12 November 2013.

Introduction

In order to increase bicycle pedaling effectiveness, it is important to be able to describe the rotation of the bicycle crank arm (Hull et al. 1991), as rotational irregularity (fluctuation of crank angular velocity) is related to pedaling efficiency (Minetti 2011). Since rotational irregularity with respect to the crank angle is not so large (Fregly et al. 2000), pedaling efficiency is reduced when rotational irregularity increases; the results of our preliminary study illustrate that this rotational irregularity is directly related to the skill of the person riding the bicycle (Kitawaki et al. 2012). Therefore, if one is able to accurately measure the rotation angle and angular velocity of the crank, it is possible to design a device that provides a measurement of the rider's skill level. Precise, high-frequency measurements of the crank angle must be made in order to accurately determine the angular velocity of the crank.

Several previous studies (Bieuzen et al. 2007; Dorel et al. 2009; Hull & Davis 1981; Hull & Jorge 1985; Chapman et al. 2006; Chapman et al. 2008; Trumbower & Faghri 2004; Gregersen et al. 2006) have measured the crank arm rotational angle on bicycle ergometers (Bieuzen et al. 2007; Dorel et al. 2009) and on road cycles (Hull & Davis 1981; Hull & Jorge 1985; Chapman et al. 2006; Chapman et al. 2008) via a potentiometer or photo encoder. However, use of potentiometers or photo encoders requires modification of the bicycle, which restricts natural measurements from ordinary bicycles. Alternatively, it is possible to use a motion capture device to measure the rotation angle of the crank arm (Trumbower & Faghri 2004; Gregersen et al. 2006); however, precise measurement of angles requires the use of expensive and large-scale systems.

In this study, we proposed an accurate measurement system for the bicycle crank angle. The system consists of small wireless motion sensor units attached to the crank arm, which have bi-axial acceleration sensors and an angular velocity sensor, which can simultaneously record the crank arm rotational angle. We evaluated the reliability and accuracy of the proposed measurement system by comparison with a motion capture device.

Materials and methods

Subjects

Twenty-four healthy adult male subjects consenting to data collection participated in the experiment, which was approved by our university ethics committee for human research. Subjects were divided into three levels according to self-reported skill level so that their mean power-to-weight ratios were equivalent to the predetermined value for each level: beginner, 1.5; intermediate, 2.25; and expert, 3.0. Table 1 shows the anthropometric (age, height, weight) and experimental (load power and power-to-weight ratio) characteristics of each group.

Experimental design

Outline of data recording system and conditions

Table 1. Anthropometric and experimental characteristics of subjects (mean ± SD).

	n=	Age (year)	Height (cm)	Weight (kg)	Power (W)	Power-to-weight ratio (W/kg)
All subjects	24	39.2 ± 7.1	171.8 ± 4.6	65.9 ± 6.4	140.4 ± 38.6	2.14 ± 0.55
Beginner	10	37.5 ± 10.0	171.7 ± 6.0	66.8 ± 6.4	105.0 ± 8.5	1.58 ± 0.07
Intermediate	9	40.9 ± 4.1	172.3 ± 3.2	64.1 ± 7.3	146.7 ± 16.6	2.29 ± 0.11
Expert	5	39.4 ± 3.6	170.8 ± 4.3	67.2 ± 5.3	200.0 ± 14.1	2.98 ± 0.08

Each subject's bicycle was attached to a bicycle trainer (Power Beam Pro: CycleOps) with a fixed rear axis. The bicycle trainer permitted the cadence to be varied while maintaining constant workload for the rider. The load for each rider was calculated by multiplying their weight and their power-to-weight ratio. The riders pedaled their bicycles for a total time of 20 minutes at their calculated load, and the last two minutes of data during these 20 minutes at which the riders pedaled at either 70 or 100 rpm were used for analysis. All measurements were collected using the data recording system illustrated in Fig. 1 and described in detail in the following paragraphs.

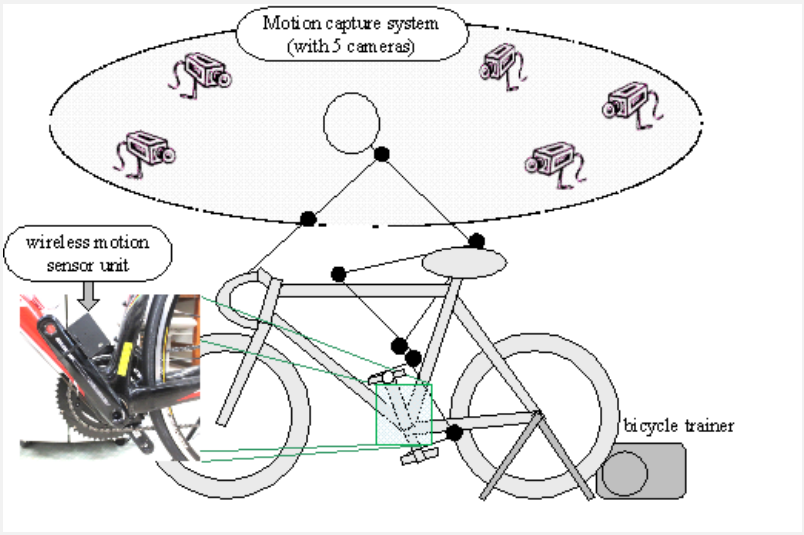

Figure 1. Overall structure of data recording system

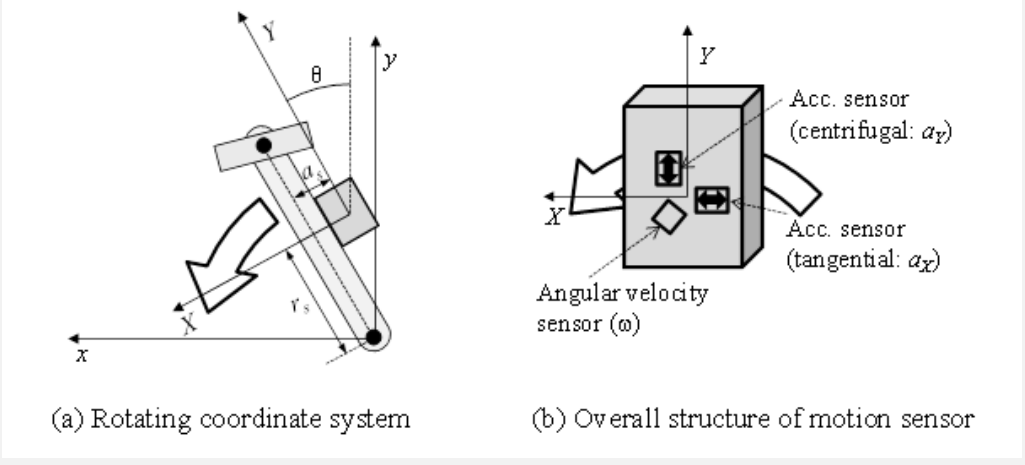

Figure 2. Rotating coordinate system and overall structure of motion sensor.

A wireless motion sensor unit (9-axis motion sensor: Logical Products) was used for data acquisition. This motion sensor was placed onto the bicycle crank arm in order to obtain the bicycle crank acceleration and angular velocity. For evaluation of the motion sensor measurements, a motion capture system (GE60/W: Library) was used as reference.

Wireless motion sensor

This experiment utilized Logical Products' 9-axis motion sensor unit, as it is commercially available. The motion sensor unit is 55 mm x 40 mm x 22 mm in size, has a weight of 35 g, and consists of the following three types of sensors: an acceleration sensor, ±50 G; an angular velocity sensor, ±1500 dps; and a magnetic sensor, ±8 Gauss. Each type of sensor was placed on each of the three coordinate axes. The motion sensor unit set on the bicycle crank arm was fixed in the X-Y rotating coordinate system, with θ defined as the rotation angle between the motion sensor X-Y coordinate system and the fixed x-y bicycle coordinate system (Fig. 2(a)). In the analysis, only bi-axial acceleration (tangential: a_X, and centrifugal: a_Y) and angular velocity (ω) obtained simultaneously by the motion sensor were used (Fig. 2(b)).

The angular velocity measured by the motion sensor is a measurement in the spatial coordinate system. However, since the bicycle body is fixed to a bicycle trainer, there is negligible movement of the bicycle relative to the spatial coordinate system. Hence, the relationship $\omega = d\theta/dt$ is satisfied. The

crank angle can be expressed by in terms of the crank angular velocity as

$$\theta(t) = \int \omega(t)dt + \theta_C \quad (1)$$

where θ_C is the initial crank angle. Using the crank angle and angular velocity, together with acceleration due to gravity (g) and the motion sensor attachment position (r_s, a_s) from the crank center, the acceleration (a_X, a_Y) of the motion sensor can be described as

$$\begin{pmatrix} a_X \\ a_Y \end{pmatrix} = \begin{pmatrix} g\sin\theta \\ g\cos\theta \end{pmatrix} - \begin{pmatrix} r_s & a_s \\ -a_s & r_s \end{pmatrix} \begin{pmatrix} \frac{d\omega}{dt} \\ \omega^2 \end{pmatrix} \quad (2)$$

The crank angle can be calculated by inserting the measured crank angular velocity into Equ. (1). By substituting the calculated crank angle and angular velocity into Equ. (2), the acceleration of the crank can be obtained. There are three parameters to be determined in these equations – the initial crank angle (θ_C) and the motion sensor attachment positions (r_s, a_s) – which can be found by minimizing the mean square error between the values of acceleration calculated using the method described above and the measured acceleration values obtained from the acceleration sensors. After finding the motion sensor attachment positions, the motion sensor was calibrated so that $\theta = 0°$ when the rotating Y-axis and the y-axis were aligned. In our proposed method, the angle of the crank arm is obtained using a motion sensor.

Motion-capture system

Reflective markers were attached to both sides of the pedal axis in order to prevent vision obstruction by the subject's leg. Five cameras – placed two on each side and one in front – were used so that the reflective markers could be captured by multiple cameras. The positions of the reflective markers were solved by motion analysis software (Move-tr/3D: Library). The calculated position of the motion capture system is a value in the spatial coordinate system. The motion capture system provides very accurate measurements. It provides position measurements within ±0.5 mm of the calibration result using reference reflective markers, and crank angle measurements within ±0.33° for the standard crank length of 170 mm.

The bicycle coordinate system was structured as shown in Fig. 3, with the z-axis passing through the center axis of the bottom bracket, the y-axis vertically upward, and the positive x-axis in the forward direction and orthogonal to the z and y-axes. The reflective markers moved along the circumference of the plane, with z-values constant in the bicycle coordinate system. The position values of the reflective markers in the spatial coordinate system, calculated by the motion capture system, were converted into the bicycle coordinate system to minimize the mean square error of the reflective marker locus on the circular movement.

As a result, the position values of reflective markers in the bicycle coordinate system – the left (Ml_x, Ml_y) and right (Mr_x, Mr_y) reflective markers – can be expressed as

$$\begin{aligned} \begin{pmatrix} Ml_x & Ml_y \end{pmatrix} &= \begin{pmatrix} r_c\sin\theta & r_c\cos\theta \end{pmatrix} \\ \begin{pmatrix} Mr_x & Mr_y \end{pmatrix} &= \begin{pmatrix} -r_c\sin\theta & -r_c\cos\theta \end{pmatrix} \end{aligned} \quad (3)$$

where r_c is the radius of the crank arm. Here, the z-axis values of the reflective markers are excluded, as they were not present in the calculation. Hence, the crank angle from the motion capture system can be obtained using the following equation:

$$\theta = \tan^{-1}\left(\frac{Ml_x - Mr_x}{Ml_y - Mr_y}\right) \quad (4)$$

Data treatment and statistical analysis

The motion sensor data was acquired at a sampling rate of 1 kHz for 25 seconds using Labview data acquisition software (National Instruments). Similarly, the motion capture system data was recorded for 25 seconds at a rate of 50 fps. The start times of the motion capture system and the motion sensor were synchronized via a hardware trigger. However, there was some time-delay in the trigger system, as the two timeframes were not perfectly synchronized. The time sequence of motion sensor data (1 kHz) was aligned with data from the motion capture system (50 fps) to reduce the RMS error values of the crank angle and angular velocity. The RMS error was calculated using the nearest motion sensor data to the time of the motion capture system.

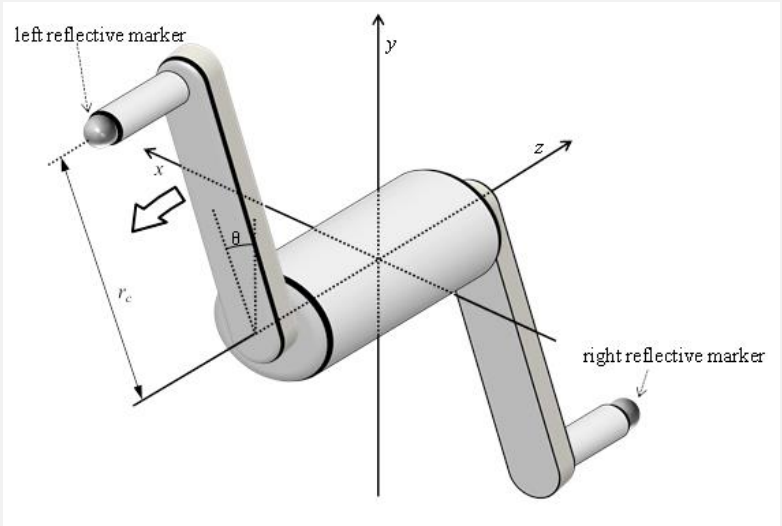

Figure 3. Bicycle coordinate system

Table 2. Comparison of motion sensor and motion capture system (mean ± SD).

	RMS error for angle (degree)		RMS error for angular velocity (%)		Correlation coefficient for angular velocity	
	70rpm	100rpm	70rpm	100rpm	70rpm	100rpm
All subjects	0.348 ± 0.157	0.330 ± 0.072	0.648 ± 0.201	0.661 ± 0.234	0.936 ± 0.070	0.907 ± 0.063
Beginner	0.388 ± 0.148	0.327 ± 0.070	0.662 ± 0.200	0.617 ± 0.240	0.946 ± 0.019	0.874 ± * 0.073
Intermediate	0.361 ± 0.188	0.332 ± 0.082	0.663 ± 0.243	0.695 ± 0.276	0.906 ± 0.108	0.931 ± 0.050
Expert	0.245 ± 0.067	0.334 ± 0.070	0.595 ± 0.141	0.688 ± 0.155	0.969 ± 0.021	0.929 ± 0.037

* $P < 0.05$

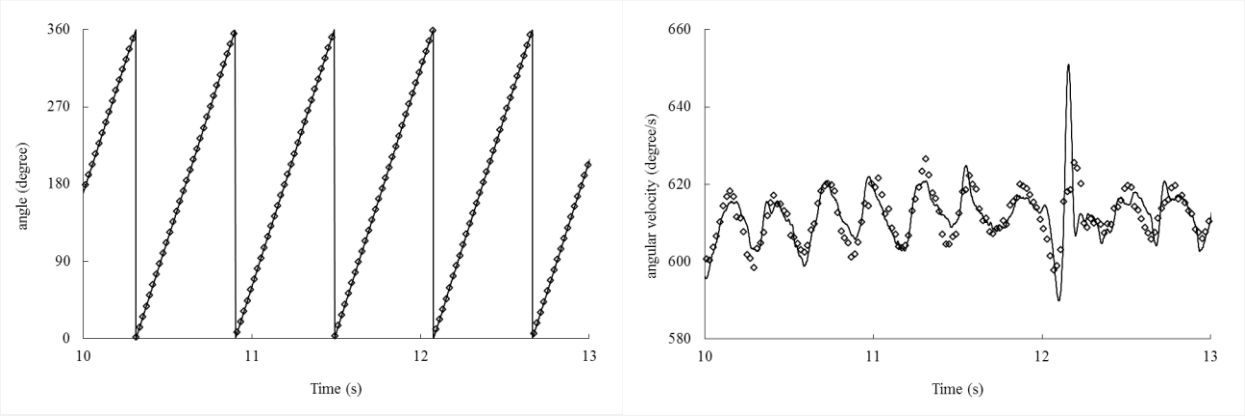

(a) crank angle (b) crank angular velocity

Figure 4. Time sequence of (a) crank angle, and (b) crank angular velocity, comparing measurements made by motion sensor (thin line) and motion capture system (circle).

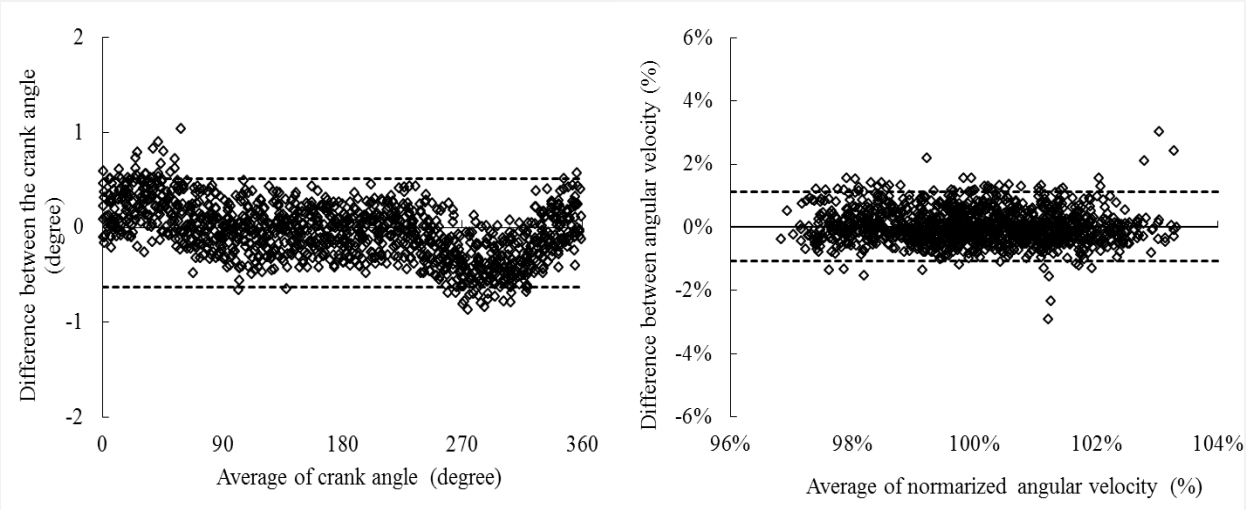

(a) Bland-Altman plot of crank angle (b) Bland-Altman plot of crank angular velocity

Figure 5. Bland Altman plot of (a) crank angle, and (b) crank angular velocity, comparing measurements made by motion sensor and motion capture system.

Statistical analysis was performed on the data, which included the determination of the RMS error values of the crank angle and the angular velocity. In addition, the Pearson's correlation coefficient of angular velocity was calculated for each of the subjects at the pedaling cadences of 70 rpm and 100 rpm. RMS errors values of the absolute crank angle were used to evaluate the absolute error of the motion sensor system. However, the RMS error values of the angular velocity were normalized by the average angular velocity, because it is angular velocity variation that indicates the rider's pedaling skill (Kitawaki et al. 2012). The effects of the subjects' levels and cadence on the RMS error values and on the correlation coefficients value were calculated using 2-factorial ANOVA (analysis of variance) individually. If there was an interaction, we analyzed a subsequent test for simple main effect. Data

were expressed as mean ± SD. $P < 0.05$ was considered statistically significant.

Results

Figure 4 provides a sample time sequence of the crank angle and the crank angular velocity. The thin lines represent the motion sensor measurements, and the circles represent the measurements of the motion capture system. Representative Bland-Altman plots of crank angle and angular velocity are shown in Fig. 5. They illustrate the measurements for one of the riders (beginner: 110 W, 100 rpm). In Fig. 6, plots of angular velocity with respect to crank angle for each subject level and cadence are shown.

Table 2 shows a comparison of the RMS errors and the correlation coefficients between the motion sensor and the motion capture system (mean ± SD). Table 3 provides the statistical results of the ANOVA and subsequent test for simple main effects. The statistical analysis illustrates that the RMS values for the angles and the angular velocities were not significantly different between subject levels or cadences. This proves that there is comparable measurement accuracy between the two measuring systems, regardless of subject level or cadence. In addition, there was a significant difference observed in correlation coefficients based on the interaction between subject levels and cadences. In subsequent test for simple main effects, there was a significant difference only for the beginners in terms of cadence conditions.

Table 3. Statistical result of the ANOVA and subsequent simple main effect.

RMS error of angle	dF	Sum Sq	Mean Sq	F value	P	partial η^2
Subject level	2	0.032	0.016	0.728	0.495	0.065
Residuals	21	0.464	0.022			
Cadence	1	0.004	0.004	0.523	0.477	0.024
Subject level x Cadence	2	0.039	0.019	2.646	0.094	0.201
Residuals	21	0.153	0.007			
RMS error of angular velocity						
Subject level	2	0.017	0.009	0.093	0.912	0.009
Residuals	21	1.925	0.092			
Cadence	1	0.002	0.002	0.203	0.657	0.010
Subject level x Cadence	2	0.035	0.017	1.747	0.199	0.143
Residuals	21	0.208	0.010			
Correlation coefficient						
Subject level	2	0.010	0.005	0.888	0.426	0.078
Residuals	21	0.120	0.006			
Cadence	1	0.010	0.010	4.171	0.054	0.166
Subject level x Cadence	2	0.023	0.011	4.710	0.020 *	0.310
Residuals	21	0.050	0.002			
Testing simple main effects of correlation coefficient of angular velocity.						
Correlation coefficient						
Subject level (70rpm)	2	0.014	0.007	1.756	0.185	0.077
Subject level (100rpm)	2	0.019	0.009	2.275	0.115	0.098
Residuals	42	0.171	0.004			
Cadence (Beginner)	1	0.026	0.026	10.821	0.003 **	0.340
Cadence (Intermediate)	1	0.003	0.003	1.161	0.293	0.052
Cadence (Expert)	1	0.004	0.004	1.608	0.219	0.071
Residuals	21	0.050	0.002			

* $P < 0.05$, ** $P < 0.01$

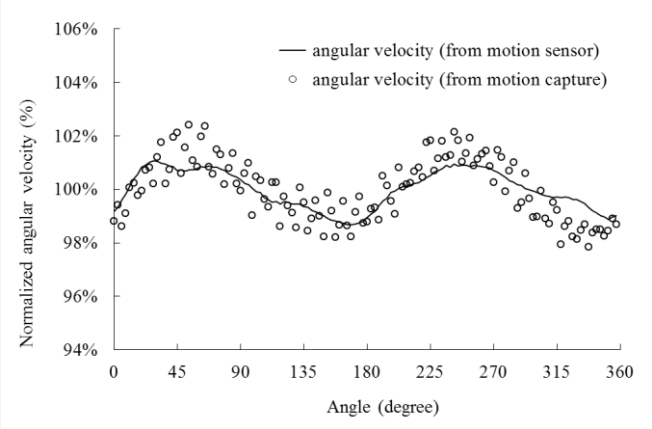

(a) Beginner, 70 rpm

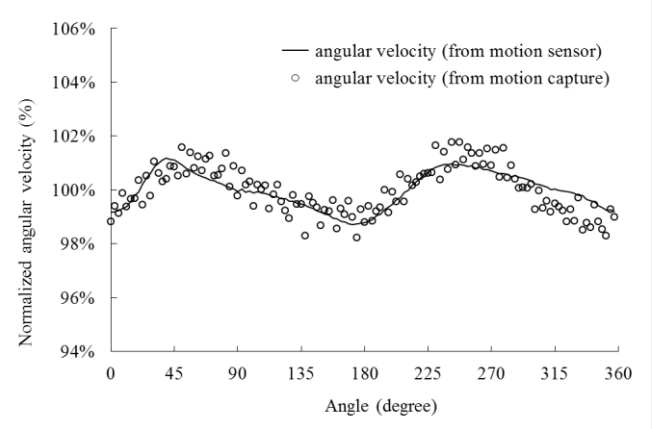

(b) Beginner, 100 rpm

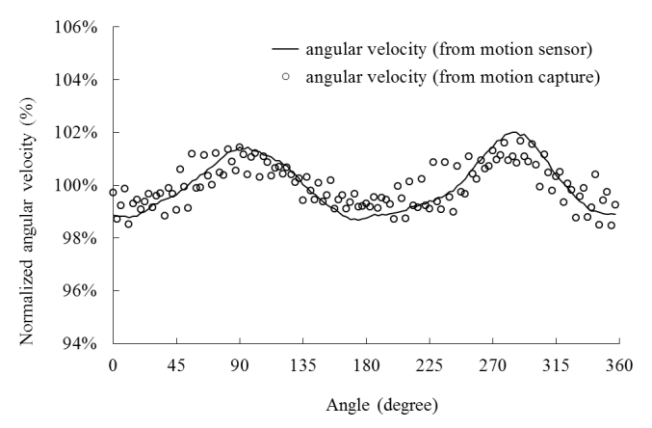

(c) Intermediate, 70 rpm

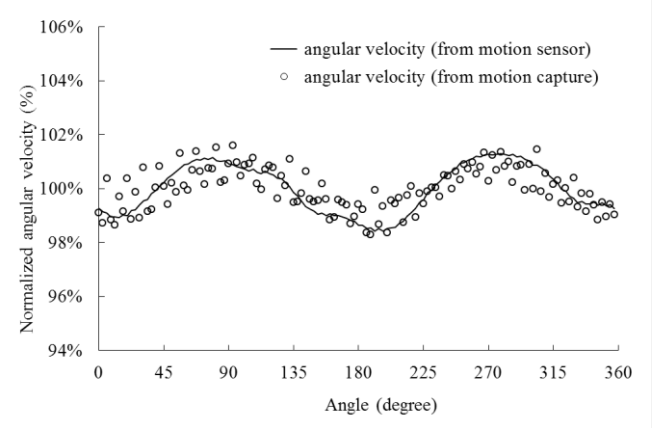

(d) Intermediate, 100 rpm

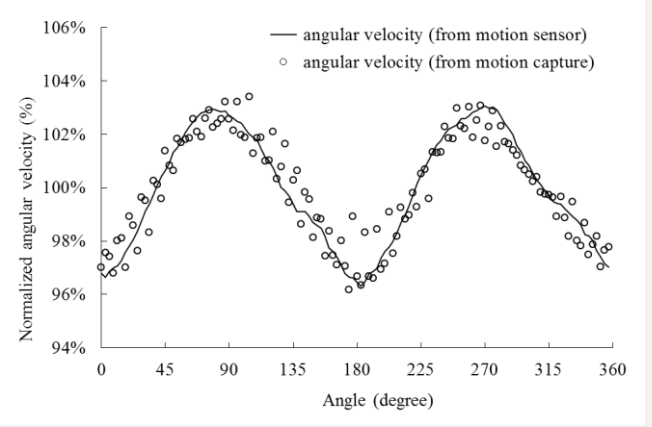

(e) Expert, 70 rpm

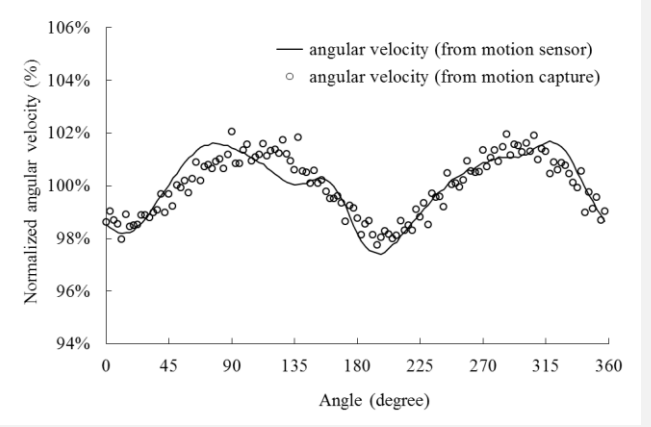

(f) Expert, 100 rpm

Figure 6. Normalized angular velocity with respect to crank angle in all conditions, comparing measurements made by motion sensor and motion capture system.

Discussion

From these results, it is evident that the obtained angle and angular velocity from both systems correlate well with each other. The validation results indicate the RMS error for the bicycle crank angle is less than 1 ° (0.339 ± 0.115 °), and that for the angular velocity to be less than 1 % (0.655 ± 0.217 %). Consequently, the time sequences of the crank arm angles and angular velocity from the motion sensor, as well as the measured sequences from the motion capture system, can be measured to the same reliability and accuracy. This means that it is possible to precisely measure the time sequence of the crank arm angles and angular velocity using only the motion sensor on the crank arm. In bicycle pedaling, the maximum variation of the angular velocity is approximately ±1.5 to 3% of the

average rotation angular velocity (Fregly et al. 2000). Considering that the measurement variance can be suppressed by averaging the measured data in the same rotational angle, as shown in Fig.6, we conclude that motion sensors make it possible to obtain precise measurements of the rotational crank angle to evaluate fluctuations in the crank angular velocity. According to Fig. 6, the angular velocity fluctuations are different depending on subject level and cadence. This means that normalized angular velocity variations may provide an indication of rider skill level. Therefore, the proposed motion sensor system may provide an alternative to expensive power meters for measuring the skill level of a rider.

The significant differences in the correlation coefficients for the beginners at different cadences are due to the fact that some beginner level subjects momentarily disengage the freewheel ratchet at 100 rpm. This phenomenon can be seen at about 12.1 seconds in Fig. 4(b). The motion sensor was able to follow the fast changes in the angular velocity, whereas large angular velocity variations are averaged by motion capture system. Hence, the RMS error for the two methods increased, while the correlation coefficient decreased. This phenomenon also appears as the difference in the high values observable in Fig. 5(b). In general, motion capture systems are quite expensive and their usage is limited to the laboratory. In addition, low frame rates means measurements cannot be high-frequency as indicated above. Therefore, using the motion sensor affords numerous advantages.

There are some limitations to the motion sensor system suggested in this study. Firstly, it can only be used in the laboratory, as it is necessary to fix the bicycle to a spatial coordinate system. If the bicycle coordinate system is variant over time (such as in various realistic environments), it would be necessary to extend the measurement system by, for example, putting another motion sensor on the bicycle frame. Secondly, the calibration scheme adopted in this study cannot be used when the bicycle is not attached to a fixed frame. When constructing a real training system, it is recommended to perform the 0° calibration in a fixed state, without moving the crank. Another limitation is the fact that when the angular velocity is small and the crank only turns a few times in the analysis interval the measurement error is increased.

In this study, we proposed a measurement system for the rotational angle of a bicycle crank arm using only a wireless motion sensor. We have drawn the following conclusions:

(1) Using the motion sensor, the rotational angle and angular velocity of the bicycle crank can be measured with the accuracy and high frequency sampling of a motion capture system.
(2) Using the motion sensor, it is possible to precisely obtain the rotational crank angle to evaluate fluctuations in crank angular velocity.

Acknowledgment

This study was subsidized by JKA through its promotion funds from KEIRIN RACE.

References

1. Bieuzen F, Lepers R, Vercruyssen F, Hausswirth C, Brisswalter J. (2007) Muscle activation during cycling at different cadences effect of maximal strength capacity. J Electromyogr Kinesiol. 17: 731-738.
2. Chapman AR, Vicenzino B, Blanch P, Knox JJ, Hodges PW. (2006) Leg muscle recruitment in highly trained cyclists. J Sports Sciences. 24: 115-124.
3. Chapman AR, Vicenzino B, Blanch P, Hodges PW. (2008) Patterns of leg muscle recruitment vary between novice and highly trained cyclists. J Electromyogr Kinesiol. 18: 359-371.
4. Dorel S, Drouet JM, Couturier A, Champoux Y, Hug F. (2009) Changes of pedaling technique and muscle coordination during an exhaustive exercise. Med Sci Sports Exerc. 41: 1277-1286.
5. Fregly BJ, Zajac FE, Dairaghi CA, (2000)Bicycle drive system dynamics: theory and experimental validation. J Biomech. Eng. 122: 446-452.
6. Gregersen CS, Hull ML, Hakansson NA. (2006) How changing the inversion/eversion foot angle affects the nondriving intersegmental knee moments and the relative activation of the vastii muscles in cycling. J Biomech. Eng. 128: 391-398.
7. Hull ML, Davis RR. (1981) Measurment of pedal loading in bicycling: I. Instrumentation. J Biomech. 14: 843-856.
8. Hull ML, Jorge M. (1985) A method for biomechanical analysis of bicycle pedaling. J Biomech. 18: 631-644.
9. Hull ML, Kautz S, Beard A. (1991) An angular velocity profile in cycling derived from mechanical energy analysis. J Biomech. 24: 577–586.
10. Kitawaki T, Oka H. (2012) Proposal of a new evaluation index of bicycle pedaling skill. 17th Annual Congress of the European College of Sport Science Book of Abstracts: 340-341.
11. Minetti AE. (2011) Bioenergetics and biomechanics of cycling: the role of 'internal work'. Eur J Appl Physiol. 111: 323-329.
12. Trumbower RD, Faghri PD. (2004) Improving pedal power during semireclined leg cycling. IEEE Eng Med Biol. 23: 62-71.